Available online at www.sciencedirect.com
SCIENCE DIRECT
International Journal of Mechanical Sciences 48 (2006) 917–925
International Journal of MECHANICAL SCIENCES
www.elsevier.com/locate/ijmecsci

Reduced dependence on loading parameters in almost conforming contacts

M. Ciavarella[a,*], A. Baldini[b], J.R. Barber[c], A. Strozzi[b]

[a]CEMEC-PoliBA - Centre of Excellence in Computational Mechanics, V.le Japigia 182, Politecnico di Bari, 70125 Bari, Italy
[b]Dipartimento di Ingegneria Meccanica e Civile Universitá degli Studi di Modena e Reggio Emilia Via Vignolese 905, Modena, Italy
[c]Department of Mechanical Engineering, University of Michigan, Ann Arbor, MI 48109-2125, USA

Received 5 September 2005; received in revised form 24 February 2006; accepted 29 March 2006

Abstract

In cases of completely conforming frictionless contact, the contact area generally either decreases or stays the same under load, in which case the extent of the contact area is subsequently independent of load and the stress and displacement fields vary linearly with the loading parameter. Dundurs and Stippes describe such cases as *receding contact problems*. Here, we demonstrate that similar results apply in the presence of Coulomb friction, in which case the extent of the stick and slip zones and the local direction of sliding are independent of load. We also show that if there is a small initial gap or interference throughout the potential contact area, the extent of the contact area and the stress and displacement fields will approach those of the corresponding receding contact problem as the applied load is increased. If the interface conditions permit adhesion between the contacting surfaces, the extent of the adhesion zone shrinks to zero as the load increases without limit. Progress of the contact configuration towards the limit is governed solely by a dimensionless load factor involving the ratio between the applied load and the initial clearance or interference. This permits results for a variety of initial geometries (due to tolerance variations) to be obtained from a set of finite element results for a single case. Some of these characteristics are demonstrated using a finite element solution of a connecting rod/bushing/gudgeon pin contact. Other interesting applications are those with complex geometries, ranging from biomechanics, as in prostheses, to the design of multiple fasteners.

Keywords: Receding contact; Conforming contact; Pinned connections; Tolerances

1. Introduction

Conforming contacts are found in a wide range of applications. Limiting the attention to pinned connection alone, the literature is replete with studies because of the extensive use of pin joints in civil, mechanical and aerospace structures and some design codes also provide useful design guides [1–4]. The elastic contact problem has also received a lot of attention from elasticians from the early days of Bickley [5] and Knight [6] who suggested simplified sinusoidal forms of pressure distribution, Howland [7], Howland and Stevenson [8] and Theocaris [9] who studied the infinite strip subject to rivet loading, and Mori [10] (the case of a semi-infinite plate). Also, several experimentalists attacked similar problems, initially by photoelastic methods [11–17] and also involving orthotropic materials [18]. This work, including more recent investigations, is reviewed by Rao [19].

Fig. 1(a) shows a frictionless elastic circular pin in a circular hole in an infinite elastic matrix, subjected to an in-plane force F. This problem was first solved by Persson [20] for the case where the materials of the pin and matrix are identical and the results are described by Johnson [21, Section 5.3]. The analysis was extended to the case of dissimilar elastic materials by Ciavarella and Decuzzi [22,23]. If the pin is an exact fit in the hole, it falls into the category described as *receding contact* by Dundurs and Stippes [24] in that the contact area decreases as soon as the load is applied and then remains constant with increasing

*Corresponding author. Tel.: +39 080 5962811; fax: +39 080 5962777.
E-mail address: mciava@poliba.it (M. Ciavarella).

0020-7403/$ - see front matter © 2006 Elsevier Ltd. All rights reserved.
doi:10.1016/j.ijmecsci.2006.03.016

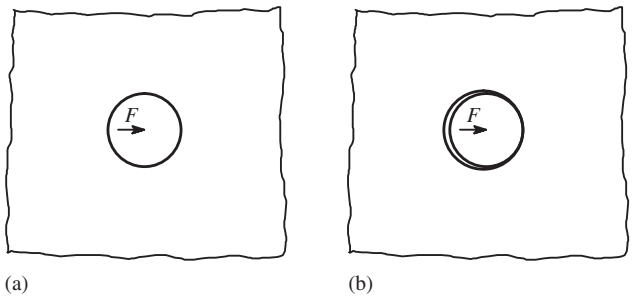

Fig. 1. A loaded elastic pin in a circular hole.

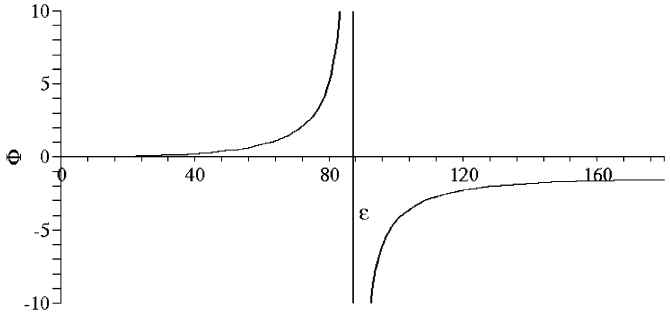

Fig. 2. Effect of the loading parameter Φ on the contact semi-angle ε.

load. Also, the stresses and displacements are everywhere proportional to the applied load. The contact configuration is shown in Fig. 1(b).

For the case with an initial clearance ΔR (or interference $-\Delta R$), Ciavarella and Decuzzi [23] showed that the applied load F and the contact semi-angle ε are related by the equation

$$\Phi \equiv \frac{F}{E'\Delta R} = \frac{\pi(\alpha+1)b^2(b^2+1)}{(\alpha-1)\left[\ln\left(\sqrt{b^2+1}\right)+2b^4\right]+2-4\beta b^2(b^2+1)}, \quad (1)$$

where $b=\tan(\varepsilon/2)$, E' is the plane strain modulus of the pin and α,β are Dundurs' bimaterial constants [25, Section 4.4.5], defined such that the pin is of material 1 and the surrounding plate of material 2. Dundurs constants are restricted to the range $-1\leqslant\alpha\leqslant 1,\ -0.5\leqslant\beta\leqslant 0.5$.

Fig. 2 shows the relationship between the applied load and the contact arc for the case of similar materials. If the pin is slightly smaller than the hole ($\Delta R>0$), contact starts from a point on the axis of symmetry in front of the load and the contact arc increases with applied load, approaching the receding contact value asymptotically at large loads. For similar materials, this limiting semi-angle is 87.46°. In Dundurs and Stippes' terminology, this is an *advancing contact* problem. Alternatively, if the pin is larger than the hole ($\Delta R<0$ and hence $\Phi<0$), axisymmetric interference stresses are developed during assembly giving a non-zero contact pressure at zero applied load. The stresses and displacements initially vary linearly with the applied load, until this is large enough to cause the contact pressure behind the load to fall to zero. This critical value corresponds to the case $b\to\infty$ ($\varepsilon=180°$) in Eq. (1) and is given by

$$\frac{F}{E'(-\Delta R)}=\frac{\pi(\alpha+1)}{2(\alpha-1)-4\beta}. \quad (2)$$

Further increase of load causes an initial rapid development of a separation arc ($d\varepsilon/d\Phi$ is unbounded at the separation point) and once again the contact arc approaches the receding contact value asymptotically at large loads, but this time from above as shown in Fig. 2. The receding contact limit for ε is shown in Fig. 3 as a function

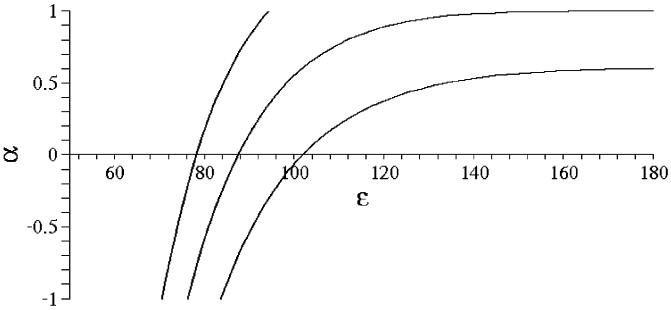

Fig. 3. Effect of Dundurs' parameter α on the receding contact semi-angle ε. The three curves, reading from left to right, are for $\beta=-0.2,0,0.2$, respectively.

of Dundurs' constant α for $\beta=-0.2,0,0.2$. In this paper, we shall demonstrate that this behaviour is characteristic of all problems of almost conforming contact. As the load is increased, the contact configuration and the stress field approach asymptotically to the solution of the corresponding receding contact problem in which the contacting bodies are completely conforming. To avoid confusion, we shall here restrict the use of the term *receding contact* to this limiting state only. Situations in which the initial contact area due to interference decreases towards the limit will be described as *regressive contact*, whilst the opposite case where the contact area grows towards the limit will be described as *progressive contact*.

2. Receding contact problems

Dundurs and Stippes [24] define a receding contact problem as one in which there are no initial stresses and the extent of the contact area Γ_C under load is included within the contact area Γ_0 at zero load—i.e. $\Gamma_C\in\Gamma_0$. The concept is further explored in Dundurs [26]. The special case where the initial contact area is retained under load ($\Gamma_C=\Gamma_0$) is defined as a *stationary contact* by Dundurs and Stippes, but Dundurs later abandoned this terminology, since all the results for receding contacts also apply to stationary contacts. However, the cases where part of the contact area ($\Gamma_0-\Gamma_C$) separates under load are more interesting, since the unilateral contact inequalities are then active in the solution.

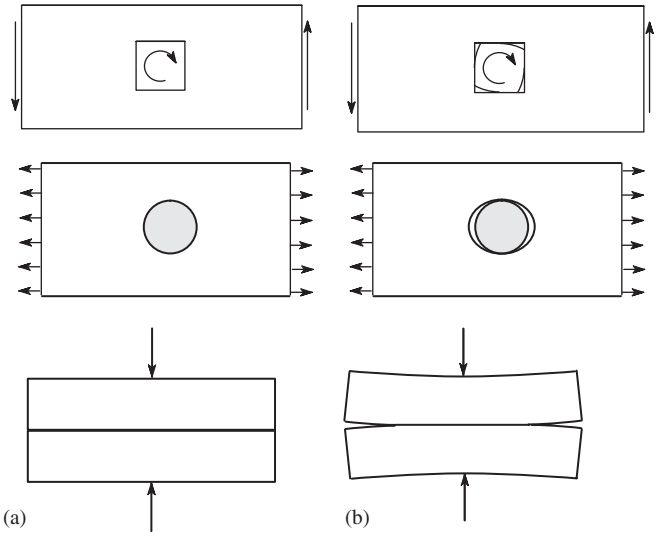

Fig. 4. Some examples of receding contact: (a) unloaded and (b) loaded configuration.

Receding contact problems necessarily fall in the category of 'conforming' contacts, since an extended contact area Γ_C must exist if a load is to be transmitted and hence Γ_0 must also be extended a fortiori. Some typical examples of receding contact problems and the corresponding loaded configurations are shown in Fig. 4. The first example shows a square peg in a square hole subjected to a twisting moment, the second shows a rigid unbounded inclusion in a bar loaded in tension and the third shows two rectangular elastic slabs compressed by equal and opposite compressive forces. This last example was first discussed by Filon [27], who already noted that separation must occur at the edges of the slab. Later Coker and Filon [11] showed by photoelastic studies that the contact semi-width is approximately 1.35 times the slab thickness. A finite element solution of this problem has since been given by Kauzlarich and Greenwood [28]. A related problem for an elastic layer pressed against an elastic substrate was treated by Keer et al. [29].

The defining characteristic of a receding contact is that the contact area decreases as soon as the load is applied and then remains constant with increasing load, during which the stresses and displacements are everywhere proportional to the applied load. These properties are easily established by writing the governing equations and the boundary conditions for the problem. The stresses $\boldsymbol{\sigma}$ and displacements $\boldsymbol{u}$ are required to satisfy the governing equations of elasticity which are here omitted in the interests of brevity. Surface tractions $\boldsymbol{\tau}$ are defined as

$$\tau_i = \sigma_{ij} n_j, \tag{3}$$

where $\boldsymbol{n}$ is the outward normal unit vector. The normal traction is then $\tau_n = \boldsymbol{\tau}.\boldsymbol{n}$ and we define the shear traction

$$\boldsymbol{\tau}_s = \boldsymbol{\tau} - \tau_n \boldsymbol{n}. \tag{4}$$

Note that in three-dimensional problems, $\boldsymbol{\tau}_s$ is a vector in the tangent plane to the local surface.

In the contact region Γ_C, $\boldsymbol{n}^{(1)} = -\boldsymbol{n}^{(2)}$ and we have

$$(\boldsymbol{u}^{(2)} - \boldsymbol{u}^{(1)}).\boldsymbol{n}^{(1)} = 0; \quad \boldsymbol{\tau}_s^{(1)} = \boldsymbol{\tau}_s^{(2)} = 0; \quad \tau_n^{(1)} = \tau_n^{(2)} \leqslant 0, \tag{5}$$

where the superscripts denote the two contacting bodies. In the region $\Gamma_0 - \Gamma_C$ that separates during loading

$$(\boldsymbol{u}^{(2)} - \boldsymbol{u}^{(1)}).\boldsymbol{n}^{(1)} \geqslant 0; \quad \boldsymbol{\tau}_s^{(1)} = \boldsymbol{\tau}_s^{(2)} = 0; \quad \tau_n^{(1)} = \tau_n^{(2)} = 0. \tag{6}$$

The inequalities in (5) and (6) state, respectively that the normal contact traction must be compressive and the gap between the separated surfaces must be positive. The remainder of the boundaries of the bodies comprise a region Γ_D, where

$$\boldsymbol{u} = \boldsymbol{U} \tag{7}$$

and a region Γ_N, where

$$\boldsymbol{\tau} = \boldsymbol{T} \tag{8}$$

and $\boldsymbol{U}, \boldsymbol{T}$ are prescribed displacements and tractions, respectively.

Suppose the solution $\boldsymbol{\sigma}, \boldsymbol{u}$ of this problem is known for some particular $\boldsymbol{U}, \boldsymbol{T}$. The governing equations and the contact boundary conditions (5)–(8) are homogeneous, so it is clear that the solution $\lambda\boldsymbol{\sigma}$, $\lambda\boldsymbol{u}$ will also satisfy these equations and correspond to proportional loading $\lambda\boldsymbol{U}$, $\lambda\boldsymbol{T}$, where λ is a scalar multiplier. Furthermore, the inequalities in (5, 6) will also be satisfied by $\lambda\boldsymbol{\sigma}$, $\lambda\boldsymbol{u}$ as long as $\lambda > 0$. Thus, the postulate that the contact area is independent of λ and the solution varies linearly with λ satisfies all the conditions of the problem and hence defines the solution, in view of the Fichera's uniqueness proof [30].

3. Coulomb friction

This elementary proof can easily be extended to the case where the contact is governed by Coulomb friction. In this case Γ_C must be divided into a slip region Γ_S and a stick region $\Gamma_C - \Gamma_S$. In Γ_S,

$$(\boldsymbol{u}^{(2)} - \boldsymbol{u}^{(1)}).\boldsymbol{n}^{(1)} = 0; \quad \tau_n^{(1)} = \tau_n^{(2)} \leqslant 0,$$

$$\boldsymbol{\tau}_s^{(1)} = -\boldsymbol{\tau}_s^{(2)} = -\frac{f(\dot{\boldsymbol{u}}^{(2)} - \dot{\boldsymbol{u}}^{(1)})\tau_n^{(1)}}{|\dot{\boldsymbol{u}}^{(2)} - \dot{\boldsymbol{u}}^{(1)}|} \tag{9}$$

and in $\Gamma_C - \Gamma_S$,

$$(\boldsymbol{u}^{(2)} - \boldsymbol{u}^{(1)}).\boldsymbol{n}^{(1)} = 0; \quad \tau_n^{(1)} = \tau_n^{(2)} \leqslant 0,$$

$$\dot{\boldsymbol{u}}^{(2)} - \dot{\boldsymbol{u}}^{(1)} = 0; \quad \boldsymbol{\tau}_s^{(1)} = -\boldsymbol{\tau}_s^{(2)}; \quad |\boldsymbol{\tau}_s^{(1)}| < -f\tau_n^{(1)}, \tag{10}$$

where the dot denotes differentiation with respect to time t. At sufficiently low loading rates, the problem can be treated as quasi-static, in which case the instantaneous loading parameter λ can be treated as a time-like variable as long as the loading is monotonic. With the postulate of linearity with λ, it then follows that $\dot{\boldsymbol{u}}^{(2)} - \dot{\boldsymbol{u}}^{(1)}$ has the same direction as $\boldsymbol{u}^{(2)} - \boldsymbol{u}^{(1)}$ and the time derivatives in (10) can be integrated from the initial condition to define the

equivalent static problem

$$(\boldsymbol{u}^{(2)}-\boldsymbol{u}^{(1)}).\boldsymbol{n}^{(1)}=0;\quad \tau_n^{(1)}=\tau_n^{(2)}\leqslant 0,$$

$$\boldsymbol{\tau}_s^{(1)}=-\boldsymbol{\tau}_s^{(2)}=-\frac{f(\boldsymbol{u}^{(2)}-\boldsymbol{u}^{(1)})\tau_n^{(1)}}{|\boldsymbol{u}^{(2)}-\boldsymbol{u}^{(1)}|} \tag{11}$$

in Γ_S and

$$(\boldsymbol{u}^{(2)}-\boldsymbol{u}^{(1)}).\boldsymbol{n}^{(1)}=0;\quad \tau_n^{(1)}=\tau_n^{(2)}\leqslant 0,$$

$$\boldsymbol{u}^{(2)}-\boldsymbol{u}^{(1)}=0;\quad \boldsymbol{\tau}_s^{(1)}=-\boldsymbol{\tau}_s^{(2)};\quad |\boldsymbol{\tau}_s^{(1)}|<-f\tau_n^{(1)}, \tag{12}$$

in $\Gamma_C-\Gamma_S$.

Suppose now that we have a solution $\boldsymbol{\sigma}$, $\boldsymbol{u}$ of (7, 8, 11, 12) for given $\boldsymbol{U}, \boldsymbol{T}$. It follows as in the frictionless case that the solution $\lambda\boldsymbol{\sigma}$, $\lambda\boldsymbol{u}$ will also satisfy (11, 12), including the inequalities and will correspond to proportional loading $\lambda\boldsymbol{U}$, $\lambda\boldsymbol{T}$. Furthermore, since $\boldsymbol{\sigma}, \boldsymbol{u}$ increase linearly with λ, it is clear that this solution also satisfies the incremental problem (9, 10). Thus, we conclude that the contact, stick and slip regions will remain unchanged throughout the loading process, as will the direction of incremental slip at any point in the slip region.[1]

4. Almost conforming contact problems

We next consider a problem that is 'almost conforming' in the sense that the initial gap between the bodies is small throughout the potential contact region. The best way to identify problems of this category is to start with a receding contact problem as defined in Section 2 and then modify it to include a small initial gap or interference between the bodies. For example, in the first case of Fig. 2, we might make the square insert slightly too large or too small for the hole in the unloaded case and in the third case, the contacting surfaces of the slabs might be slightly convex. In fact this latter case for the infinite layer was solved by Tsai et al. [31].

The corresponding frictionless contact problem can then be defined through the boundary conditions

$$(\boldsymbol{u}^{(2)}-\boldsymbol{u}^{(1)}).\boldsymbol{n}^{(1)}=-g_0;\quad \boldsymbol{\tau}_s^{(1)}=\boldsymbol{\tau}_s^{(2)}=0;\quad \tau_n^{(1)}=\tau_n^{(2)}\leqslant 0 \tag{13}$$

in Γ_C and

$$(\boldsymbol{u}^{(2)}-\boldsymbol{u}^{(1)}).\boldsymbol{n}^{(1)}\geqslant -g_0;\quad \boldsymbol{\tau}_s^{(1)}=\boldsymbol{\tau}_s^{(2)}=0;\quad \tau_n^{(1)}=\tau_n^{(2)}=0 \tag{14}$$

in $\Gamma_0-\Gamma_C$, where g_0 defines the initial gap between the bodies, which generally varies throughout Γ_0. Interference in the unloaded state is indicated by a locally negative value of g_0. The remaining boundary conditions are defined as before by Eqs. (7) and (8).

[1]Note that in the absence of a uniqueness proof for the contact problem with Coulomb friction, we cannot rule out the possibility of there being more than one solution of the problem. Indeed, if multiple solutions of (7, 8, 11, 12) exist, each of them will define a solution of the incremental problem satisfying the conditions established above.

For a given system, the stress and displacement fields depend only on the inhomogeneous terms $g_0, \boldsymbol{U}, \boldsymbol{T}$ and this dependence can be expressed symbolically in the equation

$$\boldsymbol{u}=\mathscr{F}(g_0, \boldsymbol{U}, \boldsymbol{T}), \tag{15}$$

where the function $\mathscr{F}(g_0, \boldsymbol{U}, \boldsymbol{T})$ includes information about the extent of the contact region. Consider now the field

$$\tilde{\boldsymbol{u}}=\lambda\mathscr{F}(g_0, \boldsymbol{U}, \boldsymbol{T}), \tag{16}$$

where λ is a positive scalar multiplier. It is clear that this field satisfies all the homogeneous equations and inequalities in (13, 14) and it will also satisfy the inhomogeneous conditions corresponding to a gap function λg_0 and loading $\lambda\boldsymbol{U}, \lambda\boldsymbol{T}$. It follows that

$$\lambda\mathscr{F}(g_0, \boldsymbol{U}, \boldsymbol{T})=\mathscr{F}(\lambda g_0, \lambda\boldsymbol{U}, \lambda\boldsymbol{T}). \tag{17}$$

This result is true for all $g_0, \boldsymbol{U}, \boldsymbol{T}$ and hence we can replace g_0 by g_0/λ, to obtain

$$\mathscr{F}(g_0, \lambda\boldsymbol{U}, \lambda\boldsymbol{T})=\lambda\mathscr{F}\left(\frac{g_0}{\lambda}, \boldsymbol{U}, \boldsymbol{T}\right). \tag{18}$$

If the loading parameter λ is increased without limit, we therefore have

$$\lim_{\lambda\to\infty}\frac{\mathscr{F}(g_0, \lambda\boldsymbol{U}, \lambda\boldsymbol{T})}{\lambda}=\mathscr{F}(0, \boldsymbol{U}, \boldsymbol{T}). \tag{19}$$

In other words, at sufficiently large loads, the form of the solution, including the extent of the contact area, tends to that of the corresponding receding contact problem, regardless of whether g_0 is positive (progressive contact) or negative (regressive contact). This of course is exactly the behaviour described in Section 1 for the pin-in-hole problem. The same behaviour has been reported for gudgeon pin/connecting rod ends by Parlamento [32] and for pin-lug joints by Kumar et al. [33].

4.1. Load factors and stress concentration factors

In the particular example of the pin-in-hole problem of Fig. 1, we saw that the extent of the contact area depends on the load only through the dimensionless load factor Φ, which is essentially a ratio between the applied load and a measure of the initial gap g_0. Similar results also apply to the more general problem. Suppose we define a 'normalized' gap function $\hat{g}_0$, such that

$$g_0=\alpha\hat{g}_0, \tag{20}$$

where $\hat{g}_0$ is a dimensionless function describing the shape of the gap and α is a positive scalar multiplier with dimensions of length. Substituting this result in (17) and setting $\lambda=1/\alpha$, we obtain

$$\mathscr{F}(g_0, \boldsymbol{U}, \boldsymbol{T})=\alpha\mathscr{F}\left(\hat{g}_0, \frac{\boldsymbol{U}}{\alpha}, \frac{\boldsymbol{T}}{\alpha}\right). \tag{21}$$

The function $\mathscr{F}$ defines the form of the displacement and stress fields and hence the extent of the contact area, which therefore depends only on the load factors $\boldsymbol{U}/\alpha, \boldsymbol{T}/\alpha$. For the special case of the pin-in-hole problem, the initial gap is

uniform around the circumference, so we can take $\hat{g}_0 = 1$ for progressive contact. We then have $\alpha = \Delta R$, showing that the contact semi-arc depends only on the ratio $F/\Delta R$, as is clear from Eq. (1).

The load factor can also be made dimensionless by dividing by the elastic modulus, giving for example $\Phi = F/(\alpha E)$ for two-dimensional problems, where the load F is here defined as an applied force per unit thickness. For three-dimensional problems, we would also need to introduce a length L characterizing the dimension of the components, defining $\Phi = F/(\alpha EL)$, where F now has the dimensions of force. These definitions permit generalization to classes of geometrically similar systems of various materials, assuming that Poisson's ratio is the same for all. In problems where the loading is characterized by an imposed displacement U, the appropriate loading parameter is $\Phi = U/\alpha$ for both two and three-dimensional problems.

The stress field for both progressive and regressive contact problems approaches the receding contact limit asymptotically with increasing load factor Φ and the limiting solution can be expected to provide a good approximation if Φ is large compared with unity. This behaviour is illustrated in Fig. 2, where the contact arc is within a few degrees of the limit for $|\Phi| > 10$.

In practical engineering problems, concern is generally with the highest value of some stress measure and it is conventional to define a stress concentration factor (SCF) that is the ratio of this maximum stress to some reference value that is calculated using mechanics of materials arguments. It should be clear from the above arguments that the SCF in almost conforming contact problems will tend to the receding contact limit at sufficiently large loads. Also, the SCF is a unique function of the load factor Φ. These results provide a rigorous proof of surmises of previous authors based on the results of finite element studies (e.g. Ref. [34]).

4.2. Multiple loading scenarios

In general, the externally applied traction $\boldsymbol{T}$ is a vector function of position and hence has infinitely many degrees of freedom. The scenario implied by Eq. (19) is that in which all the applied tractions increase in proportion with λ, whilst maintaining constant direction. Other more general loading scenarios might be envisaged. For example, we may start with tractions

$$\boldsymbol{T} = \boldsymbol{T}_1 + \boldsymbol{T}_2 \tag{22}$$

and then increase $\boldsymbol{T}_1$ whilst keeping $\boldsymbol{T}_2$ constant. For this case, we can write $\boldsymbol{u} = \mathscr{F}(g_0, \boldsymbol{T}_1, \boldsymbol{T}_2)$, in which case an argument analogous to that leading to (17) gives

$$\lambda\mathscr{F}(g_0, \boldsymbol{T}_1, \boldsymbol{T}_2) = \mathscr{F}(\lambda g_0, \lambda\boldsymbol{T}_1, \lambda\boldsymbol{T}_2). \tag{23}$$

Once again, this equation applies for all values of $g_0, \boldsymbol{T}_1, \boldsymbol{T}_2$, so we can replace g_0 by g_0/λ and $\boldsymbol{T}_2$ by $\boldsymbol{T}_2/\lambda$, obtaining

$$\mathscr{F}(g_0, \lambda\boldsymbol{T}_1, \boldsymbol{T}_2) = \lambda\mathscr{F}\left(\frac{g_0}{\lambda}, \boldsymbol{T}_1, \frac{\boldsymbol{T}_2}{\lambda}\right). \tag{24}$$

We then increase λ without limit, obtaining

$$\lim_{\lambda\to\infty} \frac{\mathscr{F}(g_0, \lambda\boldsymbol{T}_1, \boldsymbol{T}_2)}{\lambda} = \mathscr{F}(0, \boldsymbol{T}_1, 0). \tag{25}$$

In other words, the stress state and the contact configuration tends to the receding contact limit associated with the applied load $\boldsymbol{T}_1$ that is being increased. The load $\boldsymbol{T}_2$ that is maintained constant can be thought of as altering the initial conformity of the contact in much the same way as a change in the gap function g_0, but these effects are eventually swamped by the deformations associated with the increasing load $\boldsymbol{T}_1$.

This example also brings out the fact that the receding contact solution is a function both of the initial conforming contact geometry and the nature of the applied loading. For example, the inclusion problem of Fig. 4(a) (second example) would behave differently if subjected to biaxial instead of uniaxial loading.

4.3. Frictional problems

Similar arguments can clearly be used for the problem with Coulomb friction, showing that stick and incremental slip zones and slip directions will also tend to the values obtained in the receding contact problem at large values of λ. However the effect of the incremental friction law is qualitatively different during the evolution of progressive and regressive contact.

For regressive contact, there will initially be stick with non-zero contact pressure throughout Γ_0. In general, a finite applied load will be required to initiate slip, after which a slip zone will grow with increasing load. At some higher level of load, a separation zone will form in the slip zone and will then also grow with increasing load. In particular, regions that have once slipped will not revert to stick and hence the displacement condition in the stick zones at any stage in the loading process remains the same as at the initial zero load state (i.e. homogeneous). Thus, the boundary conditions for the problem can all be stated in terms of the instantaneous state. In fact they are the inhomogeneous equivalents of the 'static' equations (11) and (12).

By contrast, for progressive contact, the contact zone and stick zone will generally both grow with increasing load, so that there will be locations where slip gives way to stick. The displacements in the stick zones will therefore depend on the conditions at the instant when a given point made this transition and the solution is history dependent. This is a special case of the result established by Dundurs and Comninou [35] that frictional problems are history-dependent if and only if there are 'advancing stick zones'—i.e. instants at which points experience the transition from slip or separation to stick. In some special cases, the

incremental problem is self-similar, permitting a relation to be established between the progressive solution and a related stationary contact problem [36,37], but this result cannot be extended to cases where there is an inherent geometric length scale.

Note however that even in the case of progressive contacts, the configuration and stress state tends to the receding contact limit at large loads. This is because the locked in displacements in the advancing stick zones ultimately become a small proportion of the total displacements.

4.4. A brief comment about adhesion

The classical formulation of the contact problem given above assumes that no tensile tractions can be transmitted at the interface, but this is an approximation which becomes increasingly inaccurate as attention is focussed on micro and nanoscale contact. Johnson et al. [38] idealized the effect of adhesion by including the surface energy associated with the atomic potentials at the interface. The problem then becomes similar to that of linear elastic fracture mechanics (LEFM) and in particular the extent of the adhesion zone is determined by the condition that the tensile tractions be singular with a multiplier analogous to the critical stress intensity factor K_{Ic}. It is clear that the contact area in receding contact problems with adhesion cannot jump to the final value at arbitrarily small loads, since this would require the provision of a finite amount of surface energy. Furthermore, the surface energy becomes a decreasing proportion of the total strain energy as the load is increased, implying that adhesion will play a progressively smaller role in the process and the size of the adhesion zone will shrink.

If the adhesion zone is sufficiently small, its effect on the pressure distribution could be described as a local perturbation 'patched' into the asymptotic field at the edge of the contact area, where the contact pressure without adhesion has the universal form $p \sim C\sqrt{r}$ and r is the distance from the separation point. This patching technique has been successfully used for a variety of local effects in contact problems by Hills and co workers [39–41]. In the resulting asymptotic problem, the only length scale is the ratio K_{Ic}/C, from which we conclude that the extent of the adhesion zone will vary inversely with the applied load at sufficiently large loads.

5. Example

To illustrate some of these results in a practical context, we consider the automotive connecting rod/bushing/gudgeon pin assembly of Fig. 5. The diameters of the contact surfaces with appropriate tolerances are shown in Fig. 5(b). The bushing is a thin annulus which is an interference fit in the small end of the connecting rod (conrod). The gudgeon pin is a loose fit in the bushing (to allow for lubrication and relative motion). All three components are made of steel ($E = 210\,\text{GPa}$, $v = 0.3$) except that the bushing has a very thin coating of bronze alloy for tribological purposes, which was not modelled in the finite element analysis.

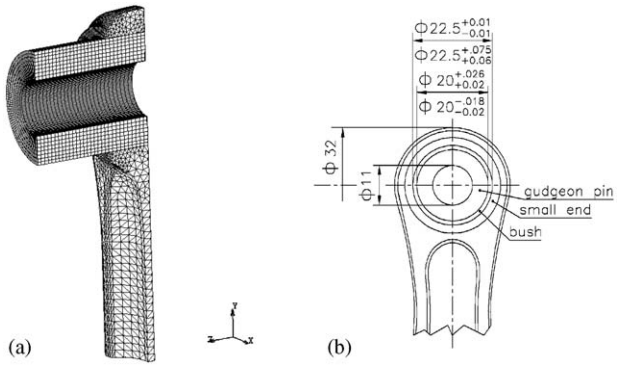

Fig. 5. The conrod/bushing/gudgeon pin assembly: (a) three-dimensional finite element mesh and (b) diameters and tolerances at the contact interfaces.

A three-dimensional finite element analysis was performed on this assembly using the mesh of Fig. 5(a), which includes about 37,000 elements and 25,000 nodes. The loading condition was chosen to be that at top dead centre (TDC) at the beginning of the induction stroke, when the small end is pulled by the maximum inertial forces exerted by the piston assembly. To mimic the actual machining and fitting of the three mechanical components, the finite element analysis included the following three steps:

(i) The bushing is press fitted into the conrod small end, using appropriate interference data from Fig. 5(b). In the calculations, we used the maximum possible diametral interference (largest bushing in smallest hole) of 0.085 mm. We also considered the case of zero interference, since this defines the receding contact limit.
(ii) Since the small end is not axisymmetric, the press fitting operation produces a small amount of ovalization of the bushing inner surface, which is therefore removed by a boring operation so as to restore a perfectly cylindrical inner surface.
(iii) The gudgeon pin is then loaded against the bushing/conrod assembly. As in step (i), we used the maximum possible diametral clearance of 0.046 mm as well as the case of zero clearance representing the receding contact limit.

The contact between the bushing and the conrod was assumed to be frictional with $f = 0.1$, whereas frictionless contact conditions were assumed at the pin/bushing interface. Loading from the piston through the contact interface between the piston bosses and the gudgeon pin was simulated by applying an appropriate uniform pressure directly to the lower portion of the pin cylindrical

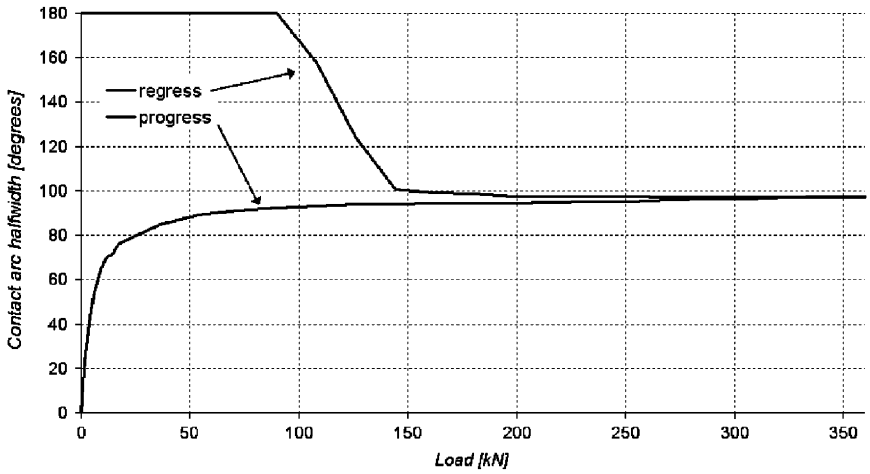

Fig. 6. Contact semi-arc at the gudgeon pin/bushing interface and the bushing/conrod interface as a function of applied load.

surface. A preliminary study in which the piston was also modelled showed this to be a satisfactory approximation.

Fig. 6 shows the contact semi-arc at both interfaces as a function of the applied load. The load is here presented in dimensional terms so that the evolution of two contact arcs can be related, but we recall that the load can be normalized in order to generate similar results for other degrees of clearance or interference. We note that the contact (progressive) arc has almost reached its receding contact limit before separation starts at the bushing/conrod interface. This is to be expected, since the design parameters should be chosen so as to preclude separation or even slip at this interface. The receding contact limit for the semi-arc was established by a separate FE calculation using zero interference and clearance and found to be 97.06° for the contact interface and 98.63° for the bushing/conrod interface.

Realistic service conditions for this problem correspond to a load of about 50 kN, from which we conclude that the bushing/conrod interface is short of the value required to cause separation (85 kN), whilst the progressive pin/bushing contact ($\varepsilon \approx 90^\circ$) is close to the receding contact limit. Note however that these calculations were performed using the maximum values of the stated tolerances. Corresponding results for smaller clearances and interferences can be calculated based on the arguments of Section 4.1. In particular, the load of 50 kN would correspond to incipient separation at the bushing/conrod interface at a load of 50 kN if the initial diametral interference were

$$\frac{0.085 \times 50}{85} = 0.050\,\text{mm},$$

and the diametral clearance at the pin/bushing interface were

$$\frac{0.046 \times 50}{85} = 0.027\,\text{mm}.$$

The critical diametral interference is just at the tolerance limit, suggesting the possibility of slip and fretting damage in this extreme case. Note also that any consequent relative rotation of the bushing and the conrod small end may close the lubrication hole and cause seizure due to oil starvation.

6. More applications

The above example illustrates one possible application of the results obtained in the paper, but is by no means exhaustive of its potentiality. In fact, the literature on conforming contact is, as seen in the introduction, very wide. In practise, most examples studied in the literature, design guides and standard codes do not recognize the linearity of the receding contact case, let alone the reduced dependence on loading. Limiting attention to the case of pinned connections, in recent years various aspects have been covered, including orthotropic materials, multiple fasteners, effect of clearance or interference, and friction [42–46,48–52]. Our results apply to all these extensions, since the only assumptions we made are those concerning small displacements at the boundary and no restrictions were placed on the material properties other than that of linear elasticity. The problem is of particular relevance in the aerospace arena, because of the wide use of fastener connection systems. Not only do the present results simplify the future analysis of these problems, but also a number of previous results can be re-interpreted for different conditions, because of the parametric dependence of load factors suggested here.

For example, in the case of multiple fasteners [47] subjected to a single type of loading, if the initial gap is the same for all contacts, and uniform around the circumference, we can still take $\hat{g}_0 = 1$ for progressive contact. We then have $\alpha = \Delta R$, showing that the contact semi-arc depends *on each contact* only on the ratio $F/\Delta R$, as is clear from Eq. (1). Hence, the problem can be studied as a function of the single load factor Φ as in our example. Separate curves will be obtained for each individual contact, but this methodology will still be very powerful

in reducing the number of runs in the typical FEM study of the problem.

A particularly interesting application is that of fretting in pinned connections. In the case of an exact fit, the problem is linear even in the presence of friction (as proved above) and the entire cycle of load can be followed easily since the extent of the stick and slip zones does not change with load, and any combination of load or traction and displacement (as is sometimes used in the analysis of fretting [45]), can be obtained immediately from a single analysis. Of course, with regressive or progressive contact, the problem ceases to be strictly linear, but the closer we are to the receding limit case, the more approximately 'linear' the problem will be, and hence we can often neglect the change of regions of contact or stick-slip.

Other possible areas of interest are those of inclusions or fiber-matrix contact where the interest is in failure [53], or in biomechanics, such as in the contact of natural or artificial joints [54,55].

7. Conclusions

We have shown that in problems of almost conforming contact, the contact area tends asymptotically to the solution of the corresponding receding contact problem—i.e. the case in which the clearance or interference is identically zero. This result also holds if Coulomb friction conditions are assumed at the interfaces, in which case the extent of the stick and slip zones also tend to the receding contact limit.

Progress of the stress state towards the limit is governed by a load factor which is a ratio between the applied load and a measure of the clearance or interference. Thus, if finite element results are obtained for a range of loads and a single value of clearance (say), results for other values of clearance can be obtained by scaling. This is useful in situations where the clearance is subject to uncertainty as is generally the case due to machining tolerances. A related useful practical result is that the stress concentration factor depends only on the load factor.

Acknowledgements

MC acknowledges funding from the Centro di Eccellenza in Meccanica Computazionale—Centre of Excellence in Computational Mechanics (CEMEC) and the PhD program in Mechanical Engineering (Ingegneria Meccanica), both directed by Prof. M. Napolitano, for sponsoring the visit to the University of Michigan, permitting also the completion of the present work.

References

[1] Blake A. Design of mechanical joints. New York: Marcel Dekker; 1985.
[2] American Institute of Steel Construction, Manual of Steel Construction, 8th ed. AISC, Chicago, 1980.
[3] American Institute of Steel Construction, Load and Resistance Factor Design, 1st ed. AISC, Chicago, 1986.
[4] American Petroleum Institute, API RP2A: Recommended Practice. (or Planning, Designing and Constructing Fixed Offshore Platforms), 18th ed. American Petroleum Institute, Dallas, 1989.
[5] Bickley WG. The distribution of stress round a circular hole in a plate. Philosophy Transactions of the Royal Society, London A 1928;221:383–415.
[6] Knight RC. The action of a rivet in a plate of finite breadth. Philosophy Magazine, Series 1935;7(19):517–40.
[7] Howland RCJ. On the stresses in the neighbourhood of a circular hole in a strip under tension. Philosophy Transactions of the Royal Society, London A 1930;229:49–86.
[8] Howland RCJ, Stevenson AC. Bi-harmonic analysis in a perforated strip. Philosophy Transactions of the Royal Society, London A 1933; 232:155–222.
[9] Theocaris PS. The stress distribution in a strip loaded in tension by means of a central pin. Transactions of ASME, Applied Mechanics 1956;78:85–90.
[10] Mori K. Stress distributions in a semi-infinite plate with a row of circular holes. Bulletin of the JSME 1972;15:899–906.
[11] Coker EG, Filon LNG. A treatise on photoelasticity. Cambridge: Cambridge University Press; 1957.
[12] Frocht MM, Hill HN. Stress-concentration factors around a central circular hole in a plate loaded through pin in the hole. Transactions of ASME Applied Mechanics 1940;62:A5–9.
[13] Frocht MM. Photoelasticity, vol. 1. New York: Wiley; 1949.
[14] Jessop HT, Snell C, Holister GS. Photoelastic investigation on plates with single interference-fit pins with load applied (a) to pin only and (b) to pin and plate simultaneously. Aeronautics Quarterly 1958;9: 147–63.
[15] Cox HL, Brown AFC. Stresses round pins in holes. Aeronautics Quarterly 1964;15:357–72.
[16] Nisida M, Saito H. Stress distributions in a semi-infinite plate due to a pin determined by interferometric method. Experimental Mechanics 1966;6:273–9.
[17] de Jong Th. Stress around pin-loaded holes in elastically orthotropic or isotropic plates. Journal of Computers and Materials 1977;11: 313–31.
[18] Hyer MW, Liu D. Stresses in pin-loaded orthotropic plates using photoelasticity. NASA contractor report, CR-172498, NASA, USA 1984.
[19] Rao AK. Elastic analysis of pin joints. Computers and Structures 1978;9:125–44.
[20] Persson A. On the stress distribution of cylindrical elastic bodies in contact, Dissertation, Chalmers Tekniska Hogskola, Göteborg, 1964.
[21] Johnson KL. Contact mechanics. Cambridge: Cambridge University Press; 1985.
[22] Ciavarella M, Decuzzi P. The state of stress induced by the plane frictionless cylindrical contact. I. The case of elastic similarity. International Journal of Solids and Structures 2001;38:4507–23.
[23] Ciavarella M, Decuzzi P. The state of stress induced by the plane frictionless cylindrical contact. II. The general case (elastic dissimilarity). International Journal of Solids and Structures 2001;38: 4525–33.
[24] Dundurs J, Stippes M. Role of elastic constants in certain contact problems. ASME Journal of Applied Mechanics 1970;37:965–70.
[25] Barber JR. Elasticity. 2nd ed. Dordrecht: Kluwer; 2002.
[26] Dundurs J. Properties of elastic bodies in contact. In: de Pater AD, Kalker JJ, editors. The mechanics of the contact between deformable bodies. Delft: Delft University Press; 1975. p. 54–66.
[27] Filon LNG. On an approximate solution for the bending of a beam of rectangular cross-section under any system of load. Philosophical Transactions of the Royal Society (London) A 1903;206:63–155.
[28] Kauzlarich JJ, Greenwood JA. Contact between a centrally loaded plate and a rigid or elastic base, with application to pivoted pad bearings. Journal of Mechanical Engineering Science 2001;215: 623–8.

[29] Keer LM, Dundurs J, Tsai KC. Problems involving a receding contact between a layer and a half-space. ASME Journal of Applied Mechanics 1972;39:1115–20.
[30] Fichera G. Boundary value problems of elasticity with unilateral constraints. In: Handbuch der Physik VI a/2. Berlin: Springer; 1972. p. 391–424.
[31] Tsai KC, Dundurs J, Keer LM. Contact between an elastic layer with a slightly curved bottom and a substrate. ASME Journal of Applied Mechanics 1972;39:821–3.
[32] Parlamento H. Exact analytical solution of the pressure distribution between gudgeon pin and conrod small end: application to the optimization of the small end geometry. PhD thesis, University of Modena, 2002.
[33] Kumar KS, Dattaguru B, Ramamurthy TS. Analysis of a cracked lug loaded by an interference fit pin. International Journal of Mechanical Sciences 1996;38:967–79.
[34] Wang GS. Stress analysis for a lug under various conditions. Journal of Strain Analysis 1994;29:7–16.
[35] Dundurs J, Comninou M. An educational elasticity problem with friction—Part I: Loading, and unloading for weak friction. ASME Journal of Applied Mechanics 1981;48:841–5.
[36] Spence DA. The Hertz problem with finite friction. Journal of Elasticity 1975;5:297–319.
[37] Storåkers B, Elaguine D. Hertz contact at finite friction and arbitrary profiles. Journal of the Mathematics and Physics of Solids 2005;53: 1422–47.
[38] Johnson KL, Kendall K, Roberts AD. Surface energy and the contact of elastic solids. Proceedings of the Royal Society (London) A 1971;324:301–13.
[39] Sackfield A, Mugadu A, Hills DA. The influence of an edge radius on the local stress field at the edge of a complete fretting contact. International Journal of Solids and Structures 2002;39:4407–20.
[40] Churchman C, Mugadu A, Hills DA. Asymptotic results for slipping complete frictional contacts. European Journal of Mechanics A/ Solids 2003;22:793–800.
[41] Dini D, Sackfield A, Hills DA. Comprehensive bounded asymptotic solutions for incomplete contacts in partial slip. Journal of the Mathematics and Physics of Solids 2005;53:437–54.
[42] Eshwar VA. Analysis of clearance fit pin joints. International Journal of Mechanical Sciences 1978;20:477–84.
[43] Wearing JL, Arnell PP, Patterson C. A study of the stress distribution in a lug loaded by a free fitting pin. Journal of Strain Analysis 1985; 20:217–24.
[44] Naik RA, Crews JH. Stress analysis method for a clearance-fit bolt under bearing loads. AIAA Journal 1986; 1348–53.
[45] Iyer K, Hahn GT, Bastias PC, Rubin CA. Analysis of fretting conditions in pinned connections. Wear 1995;181–183(2):524–30.
[46] Madenci E, Shkarayev S, Sergeev B, Oplinger DW, Shyprykevich P. Analysis of composite laminates with multiple fasteners. International Journal of Solids and Structures 1998;35(15):1793–811.
[47] Yen SW. Multirow joint fastener load investigation. Computers and Structures 1978;9(5):483–8.
[48] Ramamurthy TS. Recent studies on the behaviour of interference fit pins in composite plates. Composite Structures 1989;13(2):81–99.
[49] Ramamurthy TS. New studies on the effect of bearing loads in lugs with clearance fit pins. Composite Structures 1989;11(2): 135–50.
[50] Mangalgiri PD, Ramamurthy TS, Dattaguru B, Rao AK. Elastic analysis of pin joints in plates under some combined pin and plate loads. International Journal of Mechanical Sciences 1987;29(8): 577–85.
[51] Prabhakaran R, Naik RA. Investigation of non-linear contact for a clearance-fit bolt in a graphite/epoxy laminate. Composite Structures 1986;6(1–3):77–85.
[52] Mangalgiri PD, Dattaguru B, Rao AK. Fasteners in composite plates: effects of interfacial friction. Computers and Mathematics with Applications 1985;11(10):1057–68.
[53] Genin GM, Hutchinson JW. Failures at attachment holes in brittle matrix laminates. Journal of Composite Materials 1999;33(17):1600–19.
[54] Lewis G. Contact stress at articular surfaces in total joint replacements. Part I: Experimental methods; Part II: Analytical and numerical methods. Bio-Medical Materials and Engineering 1998; 8(2):91–110; 8(5–6):259–78.
[55] Hu XQ, Isaac GH, Fisher J. Changes in the contact area during the bedding-in wear of different sizes of metal on metal hip prostheses. Bio-Medical Materials and Engineering 2004;14(2):145–9.